Nafta-Gaz 2026, no. 1, pp. 60–66, DOI: 10.18668/NG.2026.01.06

On modeling turbulent fluid flows in concentric annular pipes

Modelowanie turbulentnych przepływów cieczy w koncentrycznych rurach pierścieniowych

Mykhaylo A. Myslyuk

Ivano-Frankivsk National Technical University of Oil and Gas

ABSTRACT: The possibility of using a rheological model of a bi-viscous fluid to describe laminar and turbulent flows of Newtonian and non-Newtonian fluids in concentric annular pipes is considered. For low shear rates, common rheological models (Newton, Bingham, Ostwald, Herschel−Bulkley, Shulman−Casson, etc.) are used, and for high shear rates, a generalization of L. Prandtl's model is applied. Considering the averaged characteristics of the flow, a model of turbulent flow and velocity distribution equations in concentric annular pipes are constructed, which ensure the continuity of the dependence of hydraulic resistance on the fluid flow rate and expand the possibilities of its application in applied problems of hydromechanics. The results of calculations of the parameters of laminar and turbulent fluid flows in concentric annular pipes for Newton, Bingham, Ostwald, Herschel−Bulkley and Shulman−Casson fluids are presented. Based on the analysis of numerical simulation results, some features of turbulent fluid flows are examined. The presence of turbulence asymmetry in concentric annular pipes is noted, which manifests itself in the occurrence of turbulent flow first in the fluid layers adjacent to the inner pipe, and then to the outer one. Critical values of the parameters (flow rate, Reynolds number) for the occurrence of turbulent flows are determined by the diameters of the annular pipes and the rheological properties of the fluid, and can differ significantly for the internal and external regions of the flow. The effect of turbulence on the removal (displacing) capacity of the fluid flow is shown.

Keywords: bi-viscous fluid; concentric annular pipes; rheological model; turbulent flow.

STRESZCZENIE: W niniejszej pracy rozważono możliwości zastosowania reologicznego modelu cieczy o zmiennej lepkości do opisu przepływów laminarnych i turbulentnych cieczy newtonowskich i nienewtonowskich w koncentrycznych rurach pierścieniowych. W przypadku niskich szybkości ścinania zastosowano typowe modele reologiczne (Newtona, Binghama, Ostwalda, Herschela–Bulkleya, Shulmana–Cassona itp.), natomiast dla wysokich szybkości ścinania wykorzystano uogólnienie modelu L. Prandtla. Na podstawie uśrednionych charakterystyk przepływu skonstruowano model przepływu turbulentnego oraz równania rozkładu prędkości w koncentrycznych przewodach pierścieniowych, które zapewniają ciągłość zależności oporu hydraulicznego od natężenia przepływu cieczy i poszerzają możliwości jego zastosowania w zagadnieniach praktycznych hydromechaniki. Przedstawiono wyniki obliczeń parametrów przepływów laminarnych i turbulentnych w koncentrycznych rurach pierścieniowych dla cieczy Newtona, Binghama, Ostwalda, Herschela–Bulkleya oraz Shulmana–Cassona. Na podstawie analizy wyników symulacji numerycznych zbadano niektóre cechy turbulentnych przepływów cieczy. Odnotowano występowanie asymetrii turbulencji w koncentrycznych rurach pierścieniowych, która objawia się występowaniem przepływu turbulentnego najpierw w warstwach cieczy przylegających do rury wewnętrznej, a następnie zewnętrznej. Wartości krytyczne parametrów (natężenia przepływu, liczby Reynoldsa) dla wystąpienia przepływów turbulentnych zależą od średnicy rur pierścieniowych oraz właściwości reologicznych cieczy i mogą znacznie różnić się dla wewnętrznych i zewnętrznych obszarów przepływu. Wykazano wpływ turbulencji na zdolność przepływu do usuwania (wypierania) materiału.

Słowa kluczowe: ciecz o zmiennej lepkości; koncentryczne rury pierścieniowe; model reologiczny; przepływ turbulentny.

Introduction

In the practice of the oil and gas industry, there is a need to model the flows of process fluids in annular pipes (Mirzajanzade et al., 1977; Mitchell, 2007; Leonov and Isaev, 2011; Lavrov and Torsaeter, 2016; Caenn et al., 2017). This is due to the problems of predicting well pressures during various process operations, assessing the removal and displacing capacity of fluids, etc. (Mirzajanzade et al., 1977; Frigaard, 2003; Mitchell, 2007; Leonov and Isaev, 2011; Lavrov and Torsaeter, 2016; Caenn et al., 2017; Frigaard and Maleki, 2018; Maleki and Frigaard, 2018; Myslyuk, 2023). Their complexity lies in modeling turbulent flows of non-Newtonian fluids with various possible rheological equations $\dot{\gamma} = \dot{\gamma}(\tau, a)$, where $\dot{\gamma}, \tau$

Corresponding author: M. Myslyuk, e-mail: *mmyslyuk@ukr.net*, *mykhailo.mysliuk@nung.edu.ua*

Article contributed to the Editor: 26.02.2025. Approved for publication: 17.12.2025.

is the velocity gradient and shear stress; a is the vector of rheological properties.

We note a fairly complete study of turbulent flows of Newtonian fluids using the Navier–Stokes equations (Reynolds, 1974; Cebeci, 2013; Loitsyanskiy, 2014; Bailly and Comte-Bellot, 2015; Kollmann, 2019; Friedrich, 2021; Galtier, 2022). In (Myslyuk, 2024), based on the rheological model of a bi-viscous fluid (Myslyuk and Salyshyn, 2008):

$$\dot{\gamma}(\tau)=\begin{cases}\dot{\gamma}_1\left(\tau,a^{(1)}\right), & \tau\le\tau^*;\\ \dot{\gamma}_2\left(\tau,a^{(2)}\right), & \tau>\tau^*,\end{cases} \tag{1}$$

a model for calculating turbulent flows in round pipes is proposed. Rheological equations $\dot{\gamma}_1\left(\tau,a^{(1)}\right)$ and $\dot{\gamma}_2\left(\tau,a^{(2)}\right)$ are used, respectively, for low (laminar flow) and high (turbulent flow) shear rates. The boundary shear stress τ^* corresponds to the actual non-trivial root of the equation $\dot{\gamma}_1\left(\tau^*,a^{(1)}\right)=\dot{\gamma}_2\left(\tau^*,a^{(2)}\right)$ and the condition of continuity of the dependence $\dot{\gamma}(\tau)$.

For low shear rates, rheological models can be used: $\dot{\gamma}_1(\tau)=\tau/\eta$ (Newton, 1999), $\dot{\gamma}_1(\tau)=(\tau-\tau_0)/\eta$ (Bingham, 1922), $\dot{\gamma}_1(\tau)=(\tau/k)^{1/n}$ (Ostwald, 1925), $\dot{\gamma}_1(\tau)=((\tau-\tau_0)/k)^{1/n}$ (Herschel and Bulkley, 1926), $\gamma_1(\tau)=(\sqrt{\tau}-\sqrt{\tau_0})^2/\eta$ (Casson, 1959), $\dot{\gamma}_1(\tau)=(\tau^{1/n}-\tau_0^{1/n})^n/\eta$ (Schulman, 1968), $\dot{\gamma}_1(\tau)=(\tau/k)^{1/n}-\beta$ (Robertson and Stiff, 1976), etc., where: η, τ_0, k, n, β are the rheological property indices.

For high shear rates, a generalization of L. Prandtl's model (Reynolds, 1974; Loitsyanskiy, 2014) has been proposed (Myslyuk, 2024) in the form:

$$\dot{\gamma}_2(\tau,a^{(2)})=\sqrt{\left(\tau-\tau_0^{(1)}\right)/\kappa^{(2)}} \tag{2}$$

where: $\tau_0^{(1)}$ is the shear yield stress for the model $\dot{\gamma}_1(\tau,a^{(1)})$; $\kappa^{(2)}$ is the index of rheological properties. At $\tau_0^{(1)}=0$, from (2) we have L. Prandtl's equation (Reynolds, 1974; Loitsyanskiy, 2014) for modeling turbulent flows of Newton and Ostwald fluids.

In (Myslyuk, 2024), the indices of rheological properties of equations $\dot{\gamma}_1(\tau,a^{(1)})$ and $\dot{\gamma}_2(\tau,a^{(2)})$ are recommended to be determined from capillary viscometry data using the principle of maximum likelihood function (Myslyuk, 1988, 2019; Myslyuk et al., 2023). Model (1), taking into account (2), according to the classification (Reynolds, 1974), refers to zero-order models and can be generalized for higher orders. Below, the features of modeling turbulent flows using (1) and (2) in concentric annular pipes are considered. Units of measurement of all physical quantities correspond to the SI system.

Turbulent flow model

The system of equations for steady flow of a bi-viscous fluid (1) and (2) in concentric annular pipes has the form (Myslyuk, 2016):

$$\begin{cases} d_2-d_1=4l\tau_0/\Delta p;\\ \tau_1=\Delta p(d_1d_2-d^2)/(4ld);\\ \tau_2=\Delta p(D^2-d_1d_2)/(4ld);\\ \Phi(d_1,d_2,\tau_1)=\Upsilon(d_1,d_2,\tau_2);\\ Q=\pi(l/\Delta p)^3[F(d_1,d_2,\tau_1)+G(d_1,d_2,\tau_2)]\end{cases} \tag{3}$$

where:

Δp – hydraulic resistance in the annular pipe over a length l,

d, D – inner and outer diameters,

d_1, d_2 – flow core diameters,

τ_1, τ_2 – shear stresses on the inner and outer walls of the pipes,

Q – fluid flow rate;

$$\Phi(d_1,d_2,\tau_1)=\begin{cases}\int\limits_{\tau_0}^{\tau_1} f(\tau,d_1,d_2)\dot{\gamma}_1(\tau,a^{(1)})d\tau, \text{ if } \tau_1\le\tau^*;\\ \int\limits_{\tau_0}^{\tau^*} f(\tau,d_1,d_2)\dot{\gamma}_1(\tau,a^{(1)})d\tau+\int\limits_{\tau^*}^{\tau_1} f(\tau,d_1,d_2)\dot{\gamma}_2(\tau,a^{(2)})d\tau, \text{ if } \tau_1>\tau^*;\end{cases}$$

$$\Upsilon(d_1,d_2,\tau_2)=\begin{cases}\int\limits_{\tau_0}^{\tau_2} h(\tau,d_1,d_2)\dot{\gamma}_1(\tau,a^{(1)})d\tau, \text{ if } \tau_2\le\tau^*;\\ \int\limits_{\tau_0}^{\tau^*} h(\tau,d_1,d_2)\dot{\gamma}_1(\tau,a^{(1)})d\tau+\int\limits_{\tau^*}^{\tau_2} h(\tau,d_1,d_2)\dot{\gamma}_2(\tau,a^{(2)})d\tau, \text{ if } \tau_2>\tau^*;\end{cases}$$

$$f(\tau,d_1,d_2)=1-\tau\Big/\sqrt{\tau^2+d_1d_2(\Delta p/2l)^2};$$

$$h(\tau,d_1,d_2)=1+\tau\Big/\sqrt{\tau^2+d_1d_2(\Delta p/2l)^2};$$

$$F(d_1,d_2,\tau_1)=\begin{cases}\int\limits_{\tau_0}^{\tau_1} \varphi(\tau,d_1,d_2)\dot{\gamma}_1(\tau,a^{(1)})d\tau, \text{ if } \tau_1\le\tau^*;\\ \int\limits_{\tau_0}^{\tau^*} \varphi(\tau,d_1,d_2)\dot{\gamma}_1(\tau,a^{(1)})d\tau+\int\limits_{\tau^*}^{\tau_1} \varphi(\tau,d_1,d_2)\dot{\gamma}_2(\tau,a^{(2)})d\tau, \text{ if } \tau_1>\tau^*;\end{cases}$$

$$G(d_1,d_2,\tau_2)=\begin{cases}\int\limits_{\tau_0}^{\tau_2} \psi(\tau,d_1,d_2)\dot{\gamma}_1(\tau,a^{(1)})d\tau, \text{ if } \tau_2\le\tau^*;\\ \int\limits_{\tau_0}^{\tau^*} \psi(\tau,d_1,d_2)\dot{\gamma}_1(\tau,a^{(1)})d\tau+\int\limits_{\tau^*}^{\tau_2} \psi(\tau,d_1,d_2)\dot{\gamma}_2(\tau,a^{(2)})d\tau, \text{ if } \tau_2>\tau^*;\end{cases}$$

$$\varphi(\tau,d_1,d_2)=\left(\tau-\sqrt{\tau^2+d_1d_2(\Delta p/2l)^2}\right)^3\Big/\sqrt{\tau^2+d_1d_2\,\Delta p/2l^2};$$

$$\psi(\tau,d_1,d_2)=\left(\tau+\sqrt{\tau^2+d_1d_2(\Delta p/2l)^2}\right)^3\Big/\sqrt{\tau^2+d_1d_2(\Delta p/2l)^2}.$$

System (3), which includes the equations of equilibrium of the flow core and on the walls of the annular pipes, the condition of equality of velocities on the inner and outer surfaces of the flow core, and the continuity equation, is convenient (τ_1, $\tau_2\ge 0$) for constructing a numerical solution $Q=A(\Delta p)$.

To construct the distribution of flow velocities, the rheology equations (1) and (2) can be used in combination with the results of solving system (3) for the inner:

$$v_1(\tau) = \begin{cases} \dfrac{l}{\Delta p}\displaystyle\int_{\tau}^{\tau_1} f(\tau,d_1,d_2)\dot{\gamma}_1(\tau,a^{(1)})d\tau, \text{ if } \tau_0 \le \tau \le \tau_1 \text{ and } \tau_1 < \tau^*; \\ \dfrac{l}{\Delta p}\left[\displaystyle\int_{\tau}^{\tau^*} f(\tau,d_1,d_2)\dot{\gamma}_1(\tau,a^{(1)})d\tau + \int_{\tau^*}^{\tau_1} f(\tau,d_1,d_2)\dot{\gamma}_2(\tau,a^{(2)})dt\right], \\ \qquad \text{if } \tau_0 \le \tau \le \tau_1 \text{ and } \tau_1 \ge \tau^*; \end{cases} \quad (4)$$

$$r_1(\tau) = \left(\sqrt{\tau^2 + d_1 d_2 (\Delta p/2l)^2} - \tau\right)(l/\Delta p),\ \tau_0 \le \tau \le \tau_1 \quad (5)$$

and external flow areas:

$$v_2(\tau) = \begin{cases} \dfrac{l}{\Delta p}\displaystyle\int_{\tau}^{\tau_2} h(\tau,d_1,d_2)\dot{\gamma}_1(\tau,a^{(1)})d\tau, \text{ if } \tau_0 \le \tau \le \tau_2 \text{ and } \tau_2 < \tau^*; \\ \dfrac{l}{\Delta p}\left[\displaystyle\int_{\tau}^{\tau^*} h(\tau,d_1,d_2)\dot{\gamma}_1(\tau,a^{(1)})d\tau + \int_{\tau^*}^{\tau_2} h(\tau,d_1,d_2)\dot{\gamma}_2(\tau,a^{(2)})d\tau\right], \\ \qquad \text{if } \tau_0 \le \tau \le \tau_2 \text{ and } \tau_2 \ge \tau^*; \end{cases} \quad (6)$$

$$r_2(\tau) = \left(\sqrt{\tau^2 + d_1 d_2 (\Delta p/2l)^2} + \tau\right)(l/\Delta p),\ \tau_0 \le \tau \le \tau_2 \quad (7)$$

where: $r_1(\tau)$, $r_2(\tau)$ are the current values of the pipe radius for the internal and external areas. The velocity of the flow core for fluids with plastic properties $\tau_0^{(1)} > 0$ is defined as $v_1(\tau_0)$ or $v_2(\tau_0)$.

In Figure 1, in accordance with (1)–(3), the dependence $\Delta p(Q)$ for the Herschel–Bulkley fluid for laminar and turbulent flows in the annular gap, as well as its rheological model $\dot{\gamma}(\tau)$, is shown as an illustration. The calculations were performed based on field data (Table 7, Myslyuk et al., 2023) of the Biocar-TF biopolymer system with a density of 1240 kg/m^3 (well 43-Semirenki, depth 5605 m) in the annular gap (D = 157.1 mm, d = 101.6 mm, l = 1000 m) for typical well designs at the Semirenky field (Raptanov et al., 2023). The rotational viscometry data were processed using the technique (Myslyuk, 1988, 2019; Myslyuk et al., 2023): shear yield stress $\tau_0^{(1)} = 2.17$ Pa , consistency index $k^{(1)} = 1.007$ Pa · s$^{0.517}$, flow index $n^{(1)} = 0.517$.

In Figure 1a, the Herschel–Bulkley fluid flow curve $\Delta p(Q)$ is constructed for the parameter $\kappa_i^{(2)} = 0{,}24262 \cdot 10^{-3}$ Pa·s^2, corresponding to the boundary shear stress $\tau^* = 20.55$ Pa. Note that the distinctive feature of the flow curves, compared to those for round pipes (Myslyuk et al., 2024), is the presence of two characteristic points for the internal $\Delta p(Q_c^{(1)})$ and external $\Delta p(Q_c^{(2)})$ flow regions, which correspond to the boundary values of the shear stresses on the pipe walls $\tau_1 = \tau^*$ and $\tau_2 = \tau^*$, as well as the critical values of the fluid flow rate $Q_c^{(1)} = 0.0089$ m^3/s and $Q_c^{(2)} = 0.0112$ m^3/s, average velocities $v_c^{(1)}$ and $v_c^{(2)}$, or Reynolds numbers $Re_c^{(1)}$ and $Re_c^{(2)}$. In quantitative terms, the difference between the critical values of flow rates $Q_c^{(1)}$ and $Q_c^{(2)}$, velocities $v_c^{(1)}$ and $v_c^{(2)}$, or Reynolds numbers $Re_c^{(1)}$ and $Re_c^{(2)}$ is determined by the diameters of the annular pipe and the indices of the rheological properties of the fluid (1). For the example considered in Figure 1, this difference is quite significant.

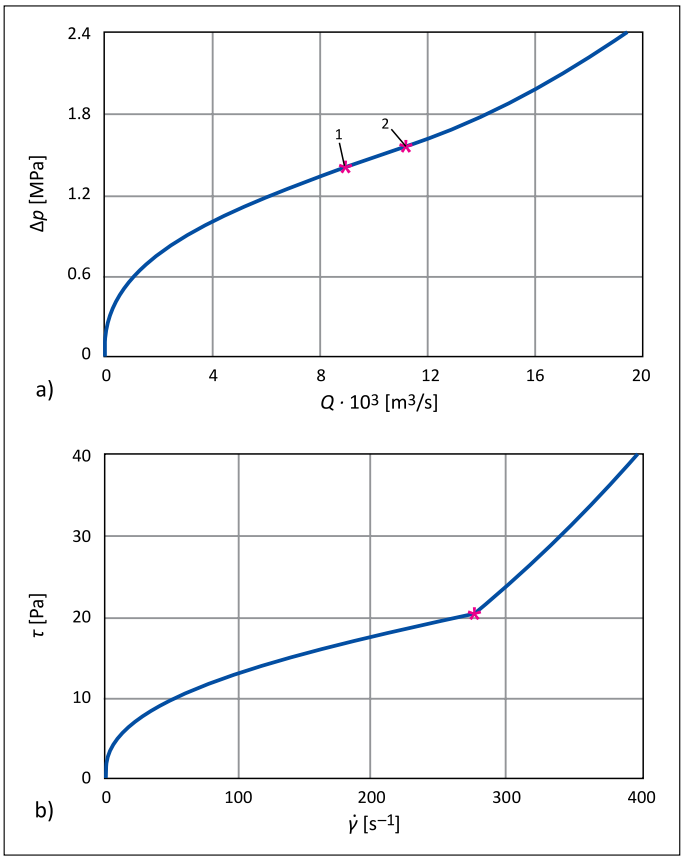

Figure 1. Herschel–Bulkley fluid flow curve in a concentric annular pipe (a) and rheological model (b): 1 – $\tau_1 = \tau^*$, 2 – $\tau_2 = \tau^*$; $\tau^* = 20.55$ Pa

Rysunek 1. Krzywa przepływu cieczy Herschela–Bulkleya w koncentrycznej rurze pierścieniowej (a) i model reologiczny (b): 1 – $\tau_1 = \tau^*$, 2 – $\tau_2 = \tau^*$, $\tau^* = 20.55$ Pa

Note that the rheological model of a bi-viscous fluid (Myslyuk et al., 2024) for concentric annular pipes indicates the occurrence of turbulence first in the inner and then in the outer regions of the flow.

Flow velocity analysis

Based on calculations using model (1)–(7), some parameters of laminar and turbulent flows of fluids of various rheological

Table 1. Density and rheological properties of drilling fluids

Tabela 1. Gęstość i właściwości reologiczne płynów wiertniczych

Drilling fluids	ρ [kg/m^3]	Rheological model	τ_0 [Pa]	$\eta(k)$ [Pa·s(Pa·s^n)]	n	$\kappa \cdot 10^3$ [Pa·s^2]
Formation water	1170	Newton	–	$0.71 \cdot 10^{-3}$	–	$3.1506 \cdot 10^{-3}$
Tamponage solution	1520	Bingham	5.18	0.0320	–	0.0831
Mineralized	1260	Ostwald	–	0.1840	0.856	1.3350
KCl Polymer	1180	Herschel-Bulkley	4.52	0.2360	0.656	0.0762
Witer II (invert emulsion)	1250	Schulman-Casson	3.28	0.0224	2.492	0.1462

models in concentric annular pipes ($D = 200$ mm, $d = 146$ mm) are considered: hydraulic resistance $\Delta p(Q)$ over a length of $l = 1000$ m; shear stresses on the walls of the inner τ_1 and outer τ_2 pipes; diameters $d_{1(2)}$ and velocities $v_{1(2)}(d_{1(2)})$ of the flow core (for Newton and Ostwald fluids, the corresponding indicators for fluid layers with maximum velocity); diameters $d^*_{i(e)}$ and velocities $v_{1(2)}(d^*_{i(e)})$ with boundary shear stress for the inner and outer regions of the flow; average flow velocity v_a; indicator of the displacing (removal) capacity of the flow $k_v = v_a / v_1(d_1)$ (Myslyuk, 2023).

Information on the density and rheological properties of some process fluids used in drilling oil and gas wells (Alboudwarej et al., 2005; Raptanov et al., 2021; Myslyuk et al., 2023; Myslyuk, 2024) is given in Table 1. Tables 2–6 present the results of calculations of the analyzed parameters of the flows of Newton, Bingham, Ostwald, Herschel–Bulkley and Shulman–Casson fluids in concentric annular gaps under laminar and turbulent conditions.

Figures 2–4 show the characteristic velocity profiles of laminar and turbulent flows of Bingham, Herschel–Bulkley, and Shulman–Casson fluids, which are constructed using model (1)–(7) for the corresponding flow rates in Tables 3, 5, and 6. Due to the symmetry of fluid flows in concentric annular pipes, Figures 2–4 show a portion of the flows for one side of the annular space, and the region of flows with high shear velocity gradients $\dot{\gamma}_2(\tau, a^{(2)})$ is highlighted (see Figures 2–4 b, c, d).

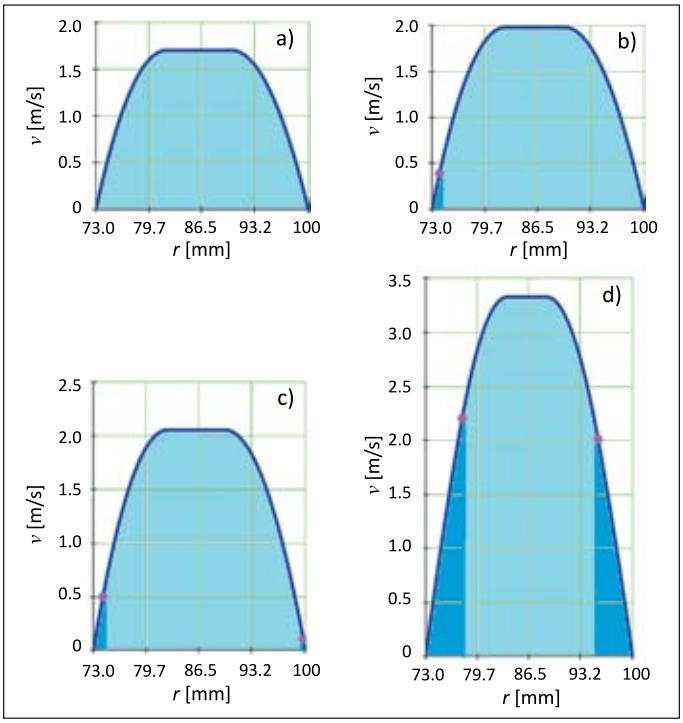

Figure 2. Distribution of Bingham fluid flow velocities in concentric annular pipes under laminar (a) $Q = 19.21 \cdot 10^{-3}$ m^3/s and turbulent (b, c, d) $Q = (22.04, 22.80, 34.79) \cdot 10^{-3}$ m^3/s regimes

Rysunek 2. Rozkład prędkości przepływu cieczy Binghama w koncentrycznych rurach pierścieniowych w warunkach laminarnych (a) $Q = 19{,}21 \cdot 10^{-3}$ m^3/s i turbulentnych (b, c, d) $Q = (22{,}04, 22{,}80, 34{,}79) \cdot 10^{-3}$ m^3/s

Table 2. Parameters of Newton fluid flow in a concentric annular pipes

Tabela 2. Parametry przepływu cieczy newtonowskich w koncentrycznych rurach pierścieniowych

$Q \cdot 10^3$ [m^3/s]	6.29	11.32	13.83	14.46	22.17	73.41
Flow regime	laminar			turbulent		
Δp [MPa]	0.005	0.009	0.011	0.0115	0.020	0.200
τ_1/τ_2 [Pa]	0.07/0.06	0.13/0.12	0.16/0.14	0.17/0.15	0.29/0.26	2.90/2.55
d_1/d_2 [mm]	172.3	172.3	172.3	172.3	172.5	172.6
$v(d_{1(2)})$ [m/s]	0.64	1.16	1.42	1.48	2.34	8.31
d_i^*/d_e^* [mm]	–	–	–	149.7/–	157.2/189.2	170.9/174.2
$v_{1(2)}(d^*_{i(e)})$ [m/s]	–	–	–	0.08/–	1.49/1.38	8.22/8.22
v_a [m/s]	0.43	0.77	0.94	0.99	1.51	5.00
k_v	0.67	0.67	0.67	0.67	0.65	0.60

– non-applicable

Analysis of the calculation results (see Tables 2–6 and Figures 2–4) indicates that the features of the kinematic characteristics of laminar and turbulent fluid flows in annular concentric and circular (Myslyuk et al., 2024) pipes are observed.

Table 3. Parameters of Bingham fluid flows in concentric annular pipes

Tabela 3. Parametry przepływu cieczy Binghama w koncentrycznych rurach pierścieniowych

$Q \cdot 10^3$ [m^3/s]	3.37	9.06	19.21	22.04	22.80	34.79
Flow regime	laminar			turbulent		
Δp [MPa]	0.625	0.865	1.252	1.360	1.390	2.000
τ_1/τ_2 [Pa]	8.70/8.25	12.16/11.32	17.73/16.30	19.31/17.67	19.75/18.05	28.71/25.75
d_1/d_2 [mm]	155.8/189.0	160.3/184.2	163.9/180.5	164.6/179.9	164.8/179.7	167.2/177.6
$v(d_{1(2)})$ [m/s]	0.26	0.76	1.71	1.98	2.05	3.33
d_i^*/d_e^* [mm]	–	–	–	147.9/–	148.4/199.5	155.5/191.0
$v_{1(2)}(d^*_{i(e)})$ [m/s]	–	–	–	0.39/–	0.50/0.10	2.20/2.01
v_a [m/s]	0.23	0.62	1.31	1.50	1.55	2.37
k_v	0.87	0.81	0.77	0.76	0.76	0.71

– non-applicable

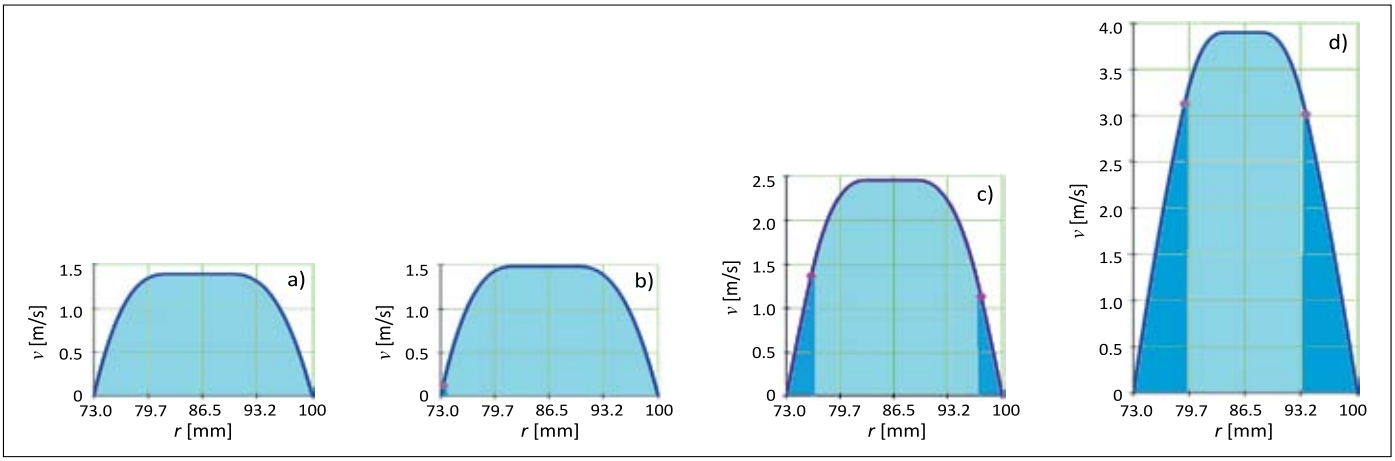

Figure 3. Distribution of Herschel–Bulkley fluid flow velocities in concentric annular pipes under laminar (a) $Q = 16.26 \cdot 10^{-3}$ m^3/s and turbulent (b, c, d) $Q = (17.28, 27.42, 40.58) \cdot 10^{-3}$ m^3/s regimes

Rysunek 3. Rozkład prędkości przepływu cieczy Herschela–Bulkleya w koncentrycznych rurach pierścieniowych w warunkach laminarnych (a) $Q = 16{,}26 \cdot 10^{-3}$ m^3/s i turbulentnych (b, c, d) $Q = (17{,}28, 27{,}42, 40{,}58) \cdot 10^{-3}$ m^3/s

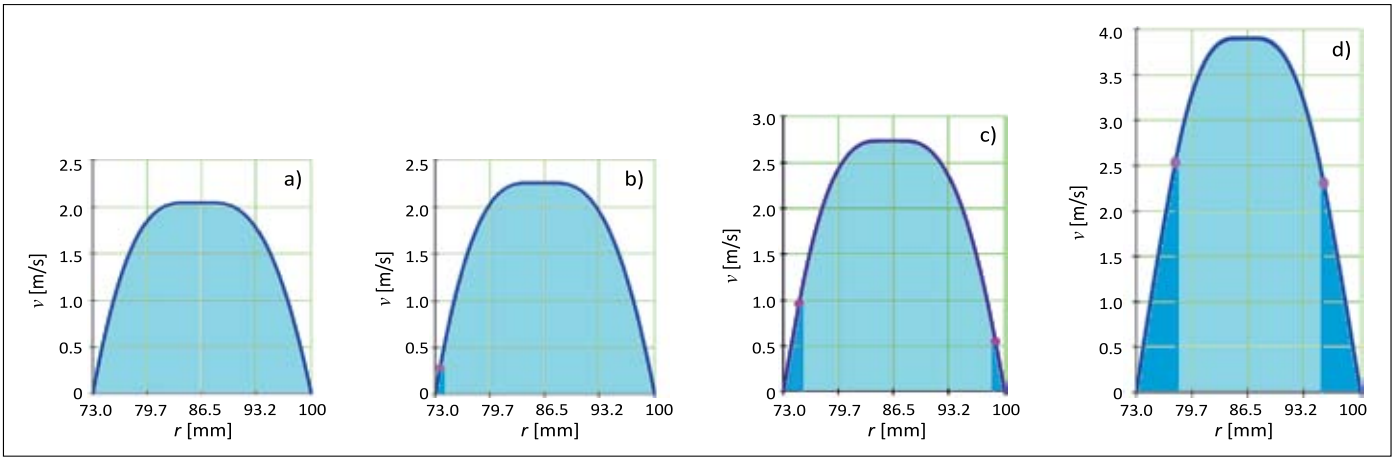

Figure 4. Distribution of Shulman–Casson fluid flow velocities in concentric annular pipes under laminar (a) $Q = 22.65 \cdot 10^{-3}$ m^3/s and turbulent (b, c, d) $Q = (24.74, 29.65, 40.47) \cdot 10^{-3}$ m^3/s regimes

Rysunek 4. Rozkład prędkości przepływu cieczy Shulmana–Cassona w koncentrycznych rurach pierścieniowych w warunkach laminarnych (a) $Q = 22{,}65 \cdot 10^{-3}$ m^3/s i turbulentnych (b, c, d) $Q = (24{,}74, 29{,}65, 40{,}47) \cdot 10^{-3}$ m^3/s

Table 4. Parameters of Ostwald fluid flows in concentric annular pipes

Tabela 4. Parametry przepływu cieczy Ostwalda w koncentrycznych rurach pierścieniowych

$Q \cdot 10^3$ [m^3/s]	3.72	4.04	4.35	4.51	5.16	17.55
Flow regime	laminar			turbulent		
Δp [MPa]	0.450	0.482	0.514	0.530	0.600	4.850
τ_1/τ_2 [Pa]	6.43/5.82	6.89/6.23	7.34/6.64	7.57/6.85	8.60/7.74	70.31/61.95
d_1/d_2 [mm]	172.2	172.2	172.2	172.2	172.3	172.6
$v(d_{1(2)})$ [m/s]	0.37	0.40	0.43	0.45	0.52	1.97
d_i^*/d_e^* [mm]	–	–	–	146.7/–	149.6/198.5	169.6/175.6
$v_{1(2)}(d^*_{i(e)})$ [m/s]	–	–	–	0.03/–	0.14/0.06	1.92/1.92
v_a [m/s]	0.25	0.28	0.30	0.31	0.35	1.20
k_v	0.68	0.68	0.68	0.68	0.68	0.61
– non-applicable						

Table 5. Parameters of Herschel-Bulkley fluid flows in a concentric annular pipes

Tabela 5. Parametry przepływu cieczy Herschela–Bulkleya w koncentrycznych rurach pierścieniowych

$Q \cdot 10^3$ [m^3/s]	2.71	9.48	16.26	17.28	27.42	40.58
Flow regime	laminar			turbulent		
Δp [MPa]	0.650	0.950	1.170	1.200	1.550	2.250
τ_1/τ_2 [Pa]	9.04/8.58	13.32/12.46	16.45/15.32	16.88/15.70	22.08/20.08	32.34/28.94
d_1/d_2 [mm]	158.2/186.1	162.5/181.5	164.3/179.7	164.5/179.5	166.4/178.1	169.0/176.2
$v(d_{1(2)})$ [m/s]	0.21	0.79	1.39	1.48	2.45	3.90
d_i^*/d_e^* [mm]	–	–	–	146.6/–	152.2/194.7	158.4 /187.6
$v_{1(2)}(d^*_{i(e)})$ [m/s]	–	–	–	0.12/–	1.36/1.13	3.13/3.01
v_a [m/s]	0.18	0.65	1.11	1.18	1.87	2.77
k_v	0.86	0.82	0.80	0.79	0.76	0.71
– non-applicable						

Table 6. Parameters of Schulman-Casson fluid flows in a concentric annular pipes

Tabela 6. Parametry przepływu cieczy Schulmana–Cassona w koncentrycznych rurach pierścieniowych

$Q \cdot 10^3$ [m^3/s]	1.38	9.26	22.65	24.74	29.65	40.47
Flow regime	laminar			turbulent		
Δp [MPa]	0.750	1.570	2.480	2.620	2.950	3.950
τ_1/τ_2 [Pa]	10.48/9.87	22.14/20.50	35.25/32.42	37.13/34.09	42.03/38.22	56.76/50.82
d_1/d_2 [mm]	163.2/180.7	167.8/176.1	169.4/174.7	169.5/174.5	169.9/174.4	170.7/174.0
$v(d_{1(2)})$ [m/s]	0.11	0.82	2.06	2.25	2.73	3.90
d_i^*/d_e^* [mm]	–	–	–	147.2/–	149.9/197.7	155.4/191.1
$v_{1(2)}(d^*_{i(e)})$ [m/s]	–	–	–	0.28/–	0.96/0.55	2.54/2.31
v_a [m/s]	0.09	0.63	1.54	1.69	2.02	2.76
k_v	0.83	0.77	0.75	0.75	0.74	0.71
– non-applicable						

Thus, with an increase in the fluid flow rate, the region of turbulent flow (rheological model $\dot{\gamma}_2(\tau, a^{(2)})$ asymptotically increases and the region of laminar flow (rheological model $\dot{\gamma}_1(\tau, a^{(1)})$) decreases; a tendency toward a decrease in the indicator k_v of the displacing capacity of the flow is observed (Myslyuk, 2023). A quantitative assessment of the displacing capacity of a flow for a given annular pipe is determined by the rheological properties and the flow rate of the fluid. For example, for a Newton fluid, the indicator k_v for a laminar flow does not depend on the flow rate and viscosity (Myslyuk, 2023), while for a turbulent flow, a characteristic decrease is observed (see Table 2).

The data in Tables 2–6 indicate a decrease in the indicator k_v for a turbulent flow within 10%.

Conclusions

1. The possibility of using bi-viscous rheological models for calculating turbulent flows of fluids in concentric annular pipes is considered. The parameters of the models are the indices of rheological properties for low and high shear rates, describing laminar and turbulent flows of fluids, respectively. It is noted that the bi-viscous model ensures the continuity of the dependence $\Delta p(Q)$ for laminar and turbulent flows, and also, due to the construction of the field of their flow velocities, expands the possibilities of application in applied problems of hydromechanics of non-Newtonian fluids.
2. It is shown that, in contrast to round pipes, asymmetry of turbulence is observed during the flow of fluids in concentric annular pipes. Turbulence first occurs in the fluid layers on the inner pipe, and then on the outer pipe. Estimates of the critical turbulence parameters (fluid flow rate, Reynolds number) depend on the pipe diameters and the rheological properties of the bi-viscous model and can differ significantly for the inner and outer flow regions.

References

Alboudwarej H., Barrere Ch.A., Hannan R.L., Archer R.A., Muhammad M., 2005. Viscosity of Formation Water: Measurement, Prediction, and Reservoir Implications. *Society of Petroleum Engineers*. DOI: 10.2118/96013-MS.

Bailly C., Comte-Bellot G., 2015. Turbulence. *Springer*. DOI: 10.1007/978-3-319-16160-0.

Bingham E.C., 1922. Fluidity and plasticity. *McGraw-Hill, New York*.

Caenn R., Darley H., Gray G., 2017. Composition and properties of drilling and completion fluids. 7 eds. *Elsevier*, DOI: 10.1016/c2015-0-04159-4.

Casson N., 1959. Flow equation for pigment oil suspensions of the printing ink type. [In:] Mills C.C. (eds.). Rheology of disperse systems. *Pergamon Press, Oxford*.

Cebeci T., 2013. Analysis of turbulent flows with computer programs. 3rd eds. Butter-Heinemann, *Elsevier Ltd*. DOI: 10.1016/C2012-0-02722-6.

Friedrich J., 2021. Non-perturbative methods in statistical descriptions of Turbulence. *Springer Cham*. DOI: 10.1007/978-3-030-51977-3.

Frigaard I.A., 2003. Predicting Transition to Turbulence in Well Construction Flows. *SPE Latin American and Caribbean Petroleum Engineering Conference, Port-of-Spain, Trinidad and Tobago*. DOI: 10.2118/81150-MS.

Frigaard I., Maleki A., 2018. Tracking fluid interface in carbon capture and storage placement application. *ASME 2018 37th International Conference on Ocean, Offshore and Arctic Engineering*. DOI: 10.1115/OMAE2018-77630.

Galtier S., 2022. Physics of wave turbulence. *Cambridge Universite Press*. DOI: 10.1017/9781009275880.

Herschel W.H., Bulkley R., 1926. Konsistenzmessungen von Gummi-Benzollösungen. *Kolloid-Zeitschrift*, 39(4): 291–300. DOI: 10.1007/BF01432034.

Kollmann W., 2019. Navier-Stokes turbulence: theory and analysis. *Springer*. DOI: 10.1007/978-3-031-59578-3.

Lavrov A., Torsaeter M., 2016. Physics and mechanics of primary well cementing. *Springer*. DOI: 10.1007/978-3-319-43165-9.

Leonov E.G., Isaev V.I., 2011. Applied hydro-aeromechanics in oil and gas drilling. *John Wiley & Sons*. DOI: 10.1002/9780470542392.

Loitsyanskiy L.G., 2014. Mechanics of liquids and gases. *Pergamon Press, Elsevier*. DOI: 10.1016/C2013-0-05328-5.

Maleki A., Frigaard I.A., 2018. Turbulent displacement flows in primary cementing of oil and gas wells. *Physics of Fluids*, 30(12): 123101. DOI: 10.1063/1.5056169.

Mirzajanzade A.Kh., Karaev A.K., Shirinzade S.A., 1977. Gidravlika v burenii i cementirovanii neftyanykh i gazovykh skvazhin. *Nedra, Moscow*.

Mitchell R.F., 2007. Petroleum engineering handbook. Volume 2. Drilling engineering. *Society of Petroleum Engineers*.

Myslyuk M.A., 1988. Determining rheological parameters for a dispersion system by rotational viscometry. *Journal of Engineering Physics and Thermophysics*, 54(6): 655−658.

Myslyuk M.A., 2016. Rheotechnologies in well drilling. *Journal of Hydrocarbon Power Engineering*, 3(2): 39−45.

Myslyuk M.A., 2019. Determination of rheological properties of drilling fluids by rotational viscometry data. *SOCAR Proceedings*, 4: 4–12. DOI: 10.5510/OGP20190400404.

Myslyuk M.A., 2023. On the assessment of the carrying capacity of drilling fluids. *SOCAR Proceedings*, 1: 26–34. DOI: 10.5510/ogp20230100801.

Myslyuk M.A., 2024. Modeling turbulent flows in round pipes. *SOCAR Proceedings*, (3): 092–097. DOI: 10.5510/OGP20240300997.

Myslyuk M., Salyzhyn Y., 2012. The evaluation of rheological parameters of non-Newtonian fluids by rotational viscosimetry. *Applied Rheology*, 22(3): 323811–323817. DOI: 3933/ApplRheol-22-32381.

Myslyuk M.A., Voloshyn Yu.D., Zholob N.R., 2023. Assesment of rheological properties of drilling fluids based on rotational viscometry data. *SOCAR Proceedings*, SI2: 41−53. DOI: 10.5510/OGP2023SI200879.

Newton I., 1999. The principia: Mathematical principles of natural philosophy. *University of California Press, Berkeley-Los Angeles-London*.

Ostwald W., 1925. Ueber die Geschwindigkeit funktion der viskosität disperser systeme. *Kolloid-Zeitschrift*, 36(2): 99–117.

Raptanov A.K., Ruzhenskyi V.V., Kostiv B.I., Myslyuk M.A., Charkovskyy V.M., 2021. Analysis of the deep drilling technology in unstable formations at the Semyrenky gas condensate field. *SOCAR Proceedings*, (SI2): 52–64. DOI: 10.5510/ogp2021si200573.

Reynolds A.J., 1974. Turbulent flows in engineering. *John Wiley & Sones*, 462.

Robertson R.E., Stiff H.A., 1976. An improved rheological model for relatings hear stress to shear rate in drilling fluids and cement slurries. *SPE Journal*, 16(1): 31–36.

Schulman Z.P., 1968. One phenomenological generalization of the flow curve of viscoplastic rheostable dispersed systems. *Proceedings of the 3rd All-Soviet Union seminar on heat and mass transfer*,10, 3–10.

Prof. Mykhailo MYSLYUK, D.Sc.
Professor of the Well Drilling Department
Ivano-Frankivsk National Technical University
of Oil and Gas
15 Karpatska Str., 76019 Ivano-Frankivsk, Ukraine
E-mail: *mykhailo.mysliuk@nung.edu.ua*